

Receptor-Ligand Interaction Between CD44 and Osteopontin (Eta-1)

Georg F. Weber,* Samy Ashkar,* Melvin J. Glimcher, Harvey Cantor

The CD44 family of surface receptors regulates adhesion, movement, and activation of normal and neoplastic cells. The cytokine osteopontin (Eta-1), which regulates similar cellular functions, was found to be a protein ligand of CD44. Osteopontin induces cellular chemotaxis but not homotypic aggregation, whereas the inverse is true for the interaction between CD44 and a carbohydrate ligand, hyaluronate. The different responses of cells after CD44 ligation by either osteopontin or hyaluronate may account for the independent effects of CD44 on cell migration and growth. This mechanism may also be exploited by tumor cells to promote metastasis formation.

The movement of lymphocytes and neoplastic cells through blood and lymphoid tissues is orchestrated by a series of interactions between cell-surface receptors and ligands contained in the extracellular matrix and on other cells (1). The CD44 receptor regulates attachment, homing, and aggregation of lymphocytes and other hematopoietic cells (2). The CD44 gene encodes a transmembrane protein that is expressed as

a family of molecular isoforms generated from alternative RNA splicing and post-translational modifications. Certain CD44 isoforms that regulate activation and migration of lymphocytes and macrophages may also enhance local growth and metastatic spread of tumor cells (3, 4). Although binding of hyaluronic acid (HA) to the NH₂-terminal domain of CD44 may enhance cellular aggregation and tumor cell growth,

this interaction does not readily account for potential CD44-dependent effects on migration and homing of normal and neoplastic cells (5).

We therefore investigated whether CD44 has another ligand. One candidate is osteopontin (Opn, also termed Eta-1, for early T lymphocyte activation 1) because of its chemotactic activity (6) and its potential role in cell attachment (7) and metastasis formation (8, 9). Opn is an extracellular phosphoprotein secreted by activated T cells as well as by osteoblasts (10), macrophages, and other cells (7, 11); several posttranslational variants of this protein have been identified (7, 12). Although Opn may interact with α_vβ₁β₃β₅-containing integrin receptors through an Arg-Gly-Asp (RGD) domain in a calcium-dependent manner (13), Opn does not always require RGD or Ca²⁺ to attach to cells (14).

Opn secreted from activated T cells displays specific and saturable binding to peritoneal monocytes and the monocyte cell line WEHI-3B (6). We confirmed that ³²P-labeled Opn, purified from K8 osteosarcoma cells (15), bound specifically to WEHI-3B cells (mean ± SEM: 40.6 ± 10.3 fmol per 10⁶ cells, of which 20.8 ± 1.7 fmol per 10⁶

Table 1. Chemotaxis of CD44 transfectants across Opn gradients. Migration of CD44-transfected (17) A31.C1 cells and A31.MLV mock-transfected cells toward K8-derived Opn was assessed by counting the numbers of cells that migrated across a polycarbonate filter after 4 hours (28). Experiment 1: Migration of CD44-transfected A31.C1 cells into lower chambers containing two concentrations of Opn (29). The migration was reduced by increasing concentrations of Opn in the upper chamber, which indicates that the response is chemotactic rather than chemokinetic. Experiments 2 and 3: Numbers of migrating A31.C1 cells (experiment 2) or A31.MLV cells (experiment 3) in chambers containing an Opn gradient. The effects of including anti-Opn or

anti-CD44 in the upper or lower chambers are shown. Osteopontin-dependent chemotaxis was noted for A31.C1 cells but not for A31.MLV cells. The migration of responding cells was inhibited by Opn antibody (rabbit immunoglobulin, 1:200 dilution) (30) or anti-CD44 KM 81 (TIB 241 supernatant, 1:200 dilution). HA did not induce A31.C1 cell migration and did not inhibit migration in response to Opn. Experiment 4: Chemotaxis of AF3.G7 cells toward recombinant Opn is dose-dependent and inhibited by Opn in the upper chamber. Hyaluronic acid did not exert chemotactic stimuli to AF3.G7 cells. Statistical significance was assessed by analysis of variance.

Lower chamber contents	Cell numbers with upper chamber contents of					Anti-Opn	Anti-CD44	HA (1 μg)
	Opn (ng)							
	0	20	50	100	200			
<i>Experiment 1: A31.C1 cells</i>								
None	38 ± 18	42 ± 21	26 ± 11	46 ± 19	19 ± 7	—	—	—
Opn (50 ng)	211 ± 36**	174 ± 48**	77 ± 24*	65 ± 12	13 ± 4	—	—	—
Opn (100 ng)	276 ± 46**	226 ± 53**	196 ± 40**	103 ± 22**	87 ± 34*	—	—	—
<i>Experiment 2: A31.C1 cells</i>								
None	15 ± 4	—	—	20 ± 8	—	11 ± 6	23 ± 7	22 ± 8
Opn (100 ng)	97 ± 32**	—	—	32 ± 13	—	67 ± 22**	43 ± 18	117 ± 28**
Anti-Opn	11 ± 4	—	—	9 ± 5	—	18 ± 7	23 ± 10	28 ± 11
Anti-CD44	17 ± 6	—	—	34 ± 11	—	26 ± 10	9 ± 4	19 ± 9
HA (1 μg)	44 ± 28	—	—	24 ± 7	—	18 ± 3	31 ± 15	21 ± 18
<i>Experiment 3: A31.MLV cells</i>								
None	21 ± 14	—	—	27 ± 11	—	10 ± 3	9 ± 3	14 ± 6
Opn (100 ng)	48 ± 22	—	—	32 ± 13	—	29 ± 12	36 ± 9	31 ± 10
Anti-Opn	9 ± 4	—	—	18 ± 8	—	11 ± 5	16 ± 5	22 ± 13
Anti-CD44	22 ± 9	—	—	24 ± 14	—	17 ± 6	8 ± 3	27 ± 13
HA (1 μg)	24 ± 8	—	—	31 ± 16	—	21 ± 8	22 ± 7	19 ± 4
<i>Experiment 4: AF3.G7 cells</i>								
None	5 ± 2	—	—	7 ± 4	4 ± 3	—	9 ± 4	—
Opn (50 ng)	48 ± 7*	—	—	21 ± 8	11 ± 6	—	15 ± 7	—
Opn (100 ng)	33 ± 11*	—	—	22 ± 6	9 ± 4	—	17 ± 8	—
HA (100 μg)	6 ± 3	—	—	5 ± 2	8 ± 3	—	2 ± 1	—

*P < 0.05. **P < 0.01.

cells remained bound in the presence of a 200-fold excess of unlabeled Opn); binding was inhibited by two rat monoclonal antibodies (mAbs) to mouse CD44 [mAb Pgp-1, clone IM7, 97%; mAb KM 81, clone TIB241, 118%; and rat immunoglobulin G (IgG), control, 19% (16)].

We also analyzed Opn binding to cellular CD44 by generating murine fibroblast A31 cell transfectants that stably expressed CD44 (A31.C1) and mock-transfected A31.MLV cells, which do not display detectable CD44 (Fig. 1A). The K8 osteosarcoma cell line, which expresses CD44 that binds to Opn in the absence of α_v and β_3 integrins [which might contribute to Opn binding (13)], was selected as the source of CD44 complementary DNA (cDNA) because these cells contain a single RNA species for CD44 as detected by polymerase chain reaction (PCR) (17). The binding of biotin-labeled Opn to A31.C1 CD44 transfectants was dependent on dose, was specific (Fig. 1B), and was inhibited by an antibody to CD44 (Fig. 1C) but not by an irrelevant antibody.

Acquisition of Opn-binding activity after stable expression of CD44 and inhibition by antibodies to CD44 suggested a direct interaction between Opn and CD44. We confirmed this by analyzing proteins that bound to recombinant glutathione-S-transferase (GST)-Opn (which lacks glycosyl moieties, including HA) immobilized on Sepharose 4B (12). Coomassie-stained electrophoresis gels of the desalted eluate showed comigration of the most prominent band with CD44 purified from the same cell line (Fig. 2A, lanes 1 and 2). Several bands of lower molecular weight were also noted, the number of which varied inversely with the stringency of the buffer conditions. The specificity of binding to immobilized Opn was confirmed by comparison of separate eluates from a GST-Opn column and a control GST column on SDS gel electrophoresis (Fig. 2A, lanes 3 and 4). The eluate from the GST-Opn column but not from the GST column contained CD44 according to protein immunoblotting with mAb KM 81 (antibody to CD44), which revealed a single band that comigrated with a KM 81-reactive band from whole AF3.G7 T cell lysate (18) and from affinity-purified CD44 on native polyacrylamide gel electrophoresis (Fig. 2B). Depletion of CD44 from cell lysates with antibody removed this band from the material eluted from the GST-Opn columns. Similar results were ob-

G. F. Weber and H. Cantor, Division of Immunopathology, Dana-Farber Cancer Institute, Department of Pathology, Harvard Medical School, Boston, MA 02115, USA. S. Ashkar and M. J. Glimcher, Department of Orthopedic Research, Children's Hospital, Harvard Medical School, Boston, MA 02115, USA.

*These authors contributed equally to this study.

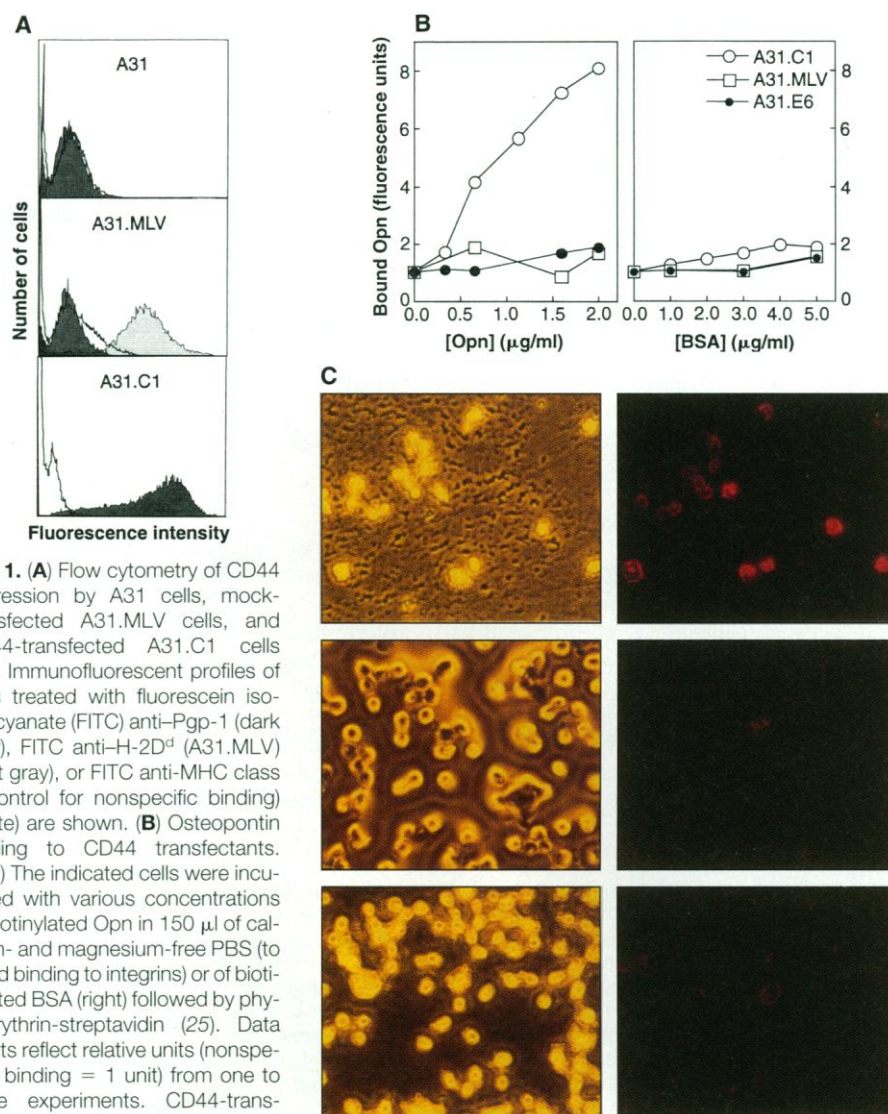


Fig. 1. (A) Flow cytometry of CD44 expression by A31 cells, mock-transfected A31.MLV cells, and CD44-transfected A31.C1 cells (24). Immunofluorescent profiles of cells treated with fluorescein isothiocyanate (FITC) anti-Pgp-1 (dark gray), FITC anti-H-2D^d (A31.MLV) (light gray), or FITC anti-MHC class II (control for nonspecific binding) (white) are shown. (B) Osteopontin binding to CD44 transfectants. (Left) The indicated cells were incubated with various concentrations of biotinylated Opn in 150 μ l of calcium- and magnesium-free PBS (to avoid binding to integrins) or of biotinylated BSA (right) followed by phycoerythrin-streptavidin (25). Data points reflect relative units (nonspecific binding = 1 unit) from one to three experiments. CD44-transfected A31.C1 cells bind in a dose-dependent manner, whereas mock-transfected A31.MLV or A31.E6 cells do not display significant binding activity. Binding does not reflect nonspecific effects associated with CD44 expression because the transfectants do not show enhanced binding to biotinylated BSA compared with the results obtained with mock-transfected A31.MLV cells. At very high concentrations of 40 μ g of BSA in 150 μ l of solution, BSA still bound equally well to A31.C1 (13.58 fluorescence units) and A31.MLV (13.60 fluorescence units) cells. (C) Fluorescence microscopy of Opn binding to CD44 transfectants. Shown are CD44-transfected A31.C1 cells (top) and mock-transfected A31.MLV cells (middle) after incubation with biotinylated Opn and addition of phycoerythrin-streptavidin as in (B). In the bottom panels, CD44⁺ A31.C1 cells were preincubated with CD44 antibody KM 81 (1:50 dilution) before analysis of binding. The isotype-matched rat antibody GK1.5 (1:50 dilution) had no effect. The left panel shows the same microscopic fields in phase contrast for comparison of cell concentration (200-fold magnification).

tained for Opn-binding material from WEHI-3B cells, K8 cells, and A31.C1 transfectants.

We next investigated the potential biological consequences of the interaction between CD44 expressed on the cell surface and the Opn ligand. Cellular adhesion participates in both cell aggregation and motility. A31.C1 cells but not A31.MLV cells adhered to plate-bound Opn or HA in calcium- and magnesium-free medium, and binding to both immobilized ligands was inhibited by soluble Opn or HA but not by

the GRGDS peptide (where G is Gly, R is Arg, D is Asp, and S is Ser) (Fig. 3). In contrast, both A31.C1 and A31.MLV cells adhered to fibronectin in calcium-containing cultures, and adherence was inhibited by the GRGDS peptide but not by HA or Opn. The efficiency of adherence to Opn and HA by A31.C1 cells was not affected by the presence or absence of calcium and magnesium. Treatment of A31.C1 cells with chondroitinase ABC did not inhibit specific binding or adherence of Opn to CD44, whereas such treatment eliminated

Fig. 2. (A) SDS-polyacrylamide gel electrophoresis (PAGE) of eluates from immobilized GST-Opn columns. GST-Opn binding material from AF3.G7 lysates is shown in lane 2 after separation on 8% SDS-PAGE followed by Coomassie staining. Co-migration with antibody-purified CD44 (KM 81, ATCC clone TIB 241) (lane 1) is apparent. Both purification procedures included pre-clearing with nonspecific affinity columns (GST for lane 2 and rat IgG for lane 1) (18). The specificity of binding was confirmed by comparison of silver-stained gels of material directly eluted from a GST-Opn column (lane 3) or a GST column (lane 4) without pre-clearing. The anti-CD44 bound material (arrowhead) represented a variant CD44 according to its size of approximately 115 kD. **(B)** Protein immunoblot analysis. Eluates from a recombinant GST-Opn column, an anti-CD44 column, and AF3.G7 whole-cell lysate were separated on native PAGE, in tris-CAPS (pH 9.4), followed by protein immunoblotting on nitrocellulose with anti-CD44 (KM 81). The visualized bands of Opn-binding material and antibody-purified CD44 co-migrated (arrowhead). Nonspecific binding was excluded because reprobing the membrane with an irrelevant antibody (rabbit IgG) did not reveal a detectable band. Opn-binding material from WEHI-3B cells, K8 cells, and A31.C1 transfectants yielded similar results.

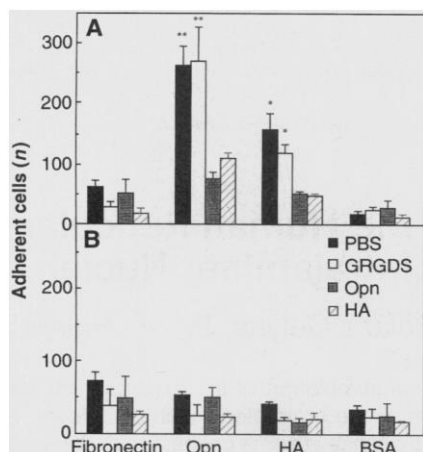
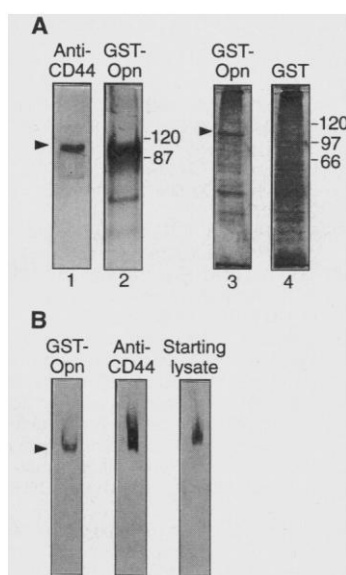


Fig. 3. Attachment of A31.C1 (A) and A31.MLV (B) cells to Opn (26). As expected (13), in the absence of divalent cations the cells did not adhere to fibronectin. Both cell lines displayed substantial adherence to fibronectin-coated plates in the presence of calcium and magnesium, an adherence that was inhibited by 1 mM GRGDS peptide but not by HA (not shown). Adherence of both A31.C1 and A31.MLV cells in calcium-containing cultures to fibronectin was inhibited by GRGDS peptide but not by HA or Opn (not shown). Statistical significance for attachment was assessed by analysis of variance; the double asterisks indicate $P < 0.01$; the single asterisk indicates $P < 0.05$.

HA-mediated aggregation and decreased attachment to HA by about 60%. These results suggest that unlike HA, Opn binding to CD44 is not mediated by chondroitin sulfate.

Because Opn can induce chemotaxis in vivo (6), we investigated whether this ligand and HA might cause CD44-dependent chemotaxis in vitro (Table 1). Transfected A31.C1 cells migrated toward Opn in modified Boyden chambers (19) in a manner reflecting chemotaxis rather than a

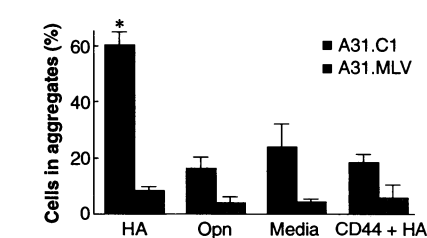


Fig. 4. Aggregation of A31.MLV or A31.C1 cells by hyaluronate and Opn (27). Addition of hyaluronate (HA; 100 $\mu\text{g/ml}$) but not Opn (Opn; 50 $\mu\text{g/ml}$) induced homotypic aggregation of CD44-transfected A31.C1 cells. Cultures of A31.C1 cells do not aggregate upon addition of anti-CD44 (25 μl of the TIB 241 supernatant) and HA (100 $\mu\text{g/ml}$) (CD44 + HA) as well as under conditions without either ligand (media). The cells were enumerated and expressed as the percentage of cells in aggregates. Approximately 200 cells per well were counted for each group for A31.C1 and A31.MLV cells. Each experiment was performed in triplicate, and each data point represents the mean of five overlapping fields. The asterisk indicates $P < 0.05$.

nonspecific increase in motility (chemokinesis) (Table 1, experiment 1) and were inhibited by antibodies to Opn or CD44 (Table 1, experiment 2). The mock-transfected cell line A31.MLV did not display chemotaxis to Opn (Table 1, experiment 3). In contrast to Opn, the CD44 ligand HA did not induce significant chemotactic activity (Table 1, experiments 2 and 3). The interaction between naturally expressed CD44 on AF3.G7 cells and Opn depicted biochemically in Fig. 2 also mediated a chemotactic response similar to that obtained after genetic transfer of CD44 into A31 cells (Table 1, experiment 4). $\alpha_v\beta_x$ integrins may also interact with Opn, and $\alpha_v\beta_3$ mediates chemotaxis of smooth muscle cells (20). Although A31 and A31.C1

cells do not express integrin $\alpha_v\beta_3$, they may express small amounts of other α_v integrins. If so, these integrins do not contribute to the Opn-dependent activation described here. CD44-negative A31.MLV cells do not bind, attach, or migrate toward Opn, and the attachment and migration of CD44⁺ A31.C1 cells is calcium-independent and inhibited by CD44 antibody but not by integrin β_3 antibody or GRGDS peptides.

HA mediates homotypic aggregation of CD44⁺ hematopoietic cells and fibroblasts (21). We confirmed that HA caused CD44⁺ A31.C1 cells, but not A31.MLV cells, to aggregate and that aggregation was inhibited completely by antibody to CD44. In contrast, Opn did not induce detectable aggregation at 10 to 100 times the concentrations necessary for attachment and chemotaxis (Fig. 4). The failure of Opn to mediate aggregation was not simply due to a small number of binding sites per molecule compared with HA because large aggregates of 5 to 10 Opn molecules are formed at the concentrations used in these experiments.

These data bring together two previously independent lines of research concerning the effects of the Opn cytokine and the CD44 receptor. The ability of Opn to regulate inflammation (6), bone formation (22), and angiogenesis (23), which has been attributed mainly to ligation of $\alpha_v\beta_3$ integrins, may also depend on an interaction with CD44. In inflammatory responses, antigen stimulation of lymphocytes leads to enhanced expression of a CD44 splice variant (3) and secretion of Opn (6, 11). Our data indicate that Opn (but not HA) can induce CD44-dependent chemotaxis (Table 1), whereas HA (but not Opn) induces CD44-dependent cell aggregation (Fig. 4). The interaction between Opn and CD44 on activated lymphocytes and monocytes may mediate migration out of the bloodstream into sites of inflammation, where additional interactions between CD44 and HA may mobilize and activate these emigrant cells.

CD44 has also been implicated in tumor metastasis (4), although its precise role in this process has been unclear. The alternative responses to CD44 ligation described above may be exploited by tumor cells to allow Opn-mediated metastatic spread and HA-dependent growth in newly colonized tissues. The definition of peptides that can block the interaction between Opn and CD44 may lead to new approaches intended to inhibit this mechanism of tumor invasion.

REFERENCES AND NOTES

1. M. C. Hu et al., *Cold Spring Harbor Symp. Quant. Biol.* **57**, 291 (1992); L. J. Picker and E. C. Butcher, *Annu. Rev. Immunol.* **10**, 561 (1992).
2. S. Huet et al., *J. Immunol.* **143**, 798 (1989); S. M. Denning et al., *ibid.* **144**, 7 (1990); B. L. Rothman et

- al., *ibid.* **147**, 2493 (1991); S. Jalkanen *et al.*, *Eur. J. Immunol.* **16**, 1195 (1986).
3. R. Arch *et al.*, *Science* **257**, 682 (1992).
 4. S. Seiter *et al.*, *J. Exp. Med.* **177**, 443 (1993); U. G. Ånther *et al.*, *Cell* **65**, 13 (1991).
 5. M. Culty *et al.*, *J. Cell Biol.* **111**, 2765 (1990).
 6. R. P. Singh *et al.*, *J. Exp. Med.* **171**, 1931 (1990).
 7. R. Patarca, R. A. Saavedra, H. Cantor, *Crit. Rev. Immunol.* **13**, 225 (1993); G. A. Rodan, *Ann. N.Y. Acad. Sci.* **760**, 1 (1995).
 8. D. T. Denhardt and X. Guo, *FASEB J.* **7**, 1475 (1993).
 9. D. R. Senger, C. A. Perruzzi, A. Papadopoulos, *Anticancer Res.* **9**, 1291 (1989); A. M. Craig *et al.*, *Int. J. Cancer* **46**, 133 (1990); A. F. Chambers *et al.*, *Anticancer Res.* **12**, 43 (1992); E. I. Behrend *et al.*, *Cancer Res.* **54**, 832 (1994).
 10. M. D. McKee *et al.*, *Anat. Rec.* **228**, 77 (1990); M. D. McKee, M. J. Glimcher, A. Nanci, *ibid.* **234**, 479 (1992).
 11. R. Patarca *et al.*, *J. Exp. Med.* **170**, 145 (1989).
 12. S. Ashkar *et al.*, *Biochem. Biophys. Res. Commun.* **191**, 126 (1993).
 13. A. Oldberg, A. Franzen, D. Heinegard, *Proc. Natl. Acad. Sci. U.S.A.* **83**, 8819 (1986); A. Oldberg *et al.*, *J. Biol. Chem.* **263**, 19433 (1988); M. Sato *et al.*, *J. Cell Biol.* **111**, 1713 (1990); L. Liaw *et al.*, *J. Clin. Invest.* **95**, 713 (1995).
 14. S. van Dijk *et al.*, *J. Bone Miner. Res.* **8**, 1499 (1993).
 15. K8 cells are differentiated osteosarcoma cells that display high metastatic activity and secrete large amounts of Opn [O. Aresu *et al.*, *Invasion Metastasis* **11**, 2 (1991); J. Schmidt *et al.*, *Differentiation* **39**, 151 (1988)], which is O-glycosylated, not N-glycosylated, contains eight phosphates per mole of protein, and does not express detectable hyaluronate. Osteopontin purified from K8 supernatants by antibody-dependent affinity chromatography was homogenous according to NH₂-terminal sequence analysis.
 16. Two and a half picomoles of ³²P-labeled immunofluorescence-purified Opn from K8 cells was added to 1 × 10⁶ WEHI-3B cells (about half the saturating concentration), incubated at room temperature in the presence or absence of antibody to CD44 (anti-CD44) or control antibody [mAb Pgp-1, clone IM7 from Pharmingen; mAb KM 81, clone TIB241 from the American Type Culture Collection (ATCC); and rat IgG from Sigma] at 3 μg or a 200-fold excess of unlabeled Opn in 250 μl before bound and free fractions were separated by centrifugation as described (6) in four separate experiments. Similar results were obtained for binding of recombinant phosphorylated Opn to K8 cells.
 17. CD44 was expressed in the murine embryonic cell line A31 after amplification of cDNA from K8 cells with 5'-CAGAATTCCTCGATCTCCTGGTAAGGAG-3' and 5'-TAGGATCCTGCCTCAACTGTGCACTCA-3' primers, resulting in a single species of cDNA containing exons 7v through 10v according to PCR and sequencing analysis. This cDNA was cloned into the Bam HI-Eco RI sites of the eukaryotic expression vector pcDNA III/neo (Invitrogen, San Diego CA), which contains enhancer-promoter sequences from the early gene of human cytomegalovirus, the SV40 polyadenylation-transcription termination signal, and the neomycin resistance gene for selection. CD44 clones were transfected into the A31 mouse embryonic fibroblast cell line by electroporation and selection according to G418 resistance and adherence to HA.
 18. The AF3.G7 hybridoma, generated by fusing cow insulin-immune C57BL/6 lymph node cells with the BW5147 thymoma line, responds to cow insulin according to interleukin-2 production [D. G. Spinella *et al.*, *J. Immunol.* **138**, 3991 (1987)] and expresses CD44 on its cell surface as judged by flow cytometry analysis with Pgp-1 antibody (clone IM7, Pharmingen). AF3.G7 cells were lysed in 0.1% Triton X-100 buffer containing 25 mM potassium phosphate, pH 7.4, 4 mM EDTA, 10 mM sodium chloride, 5 mM magnesium chloride, 10 mM iodoacetamide, 0.025% (w/v) sodium azide, 0.2 U/ml of aprotinin, 20 mg/ml of pepstatin A, 1 mM phenylmethylsulfonyl fluoride, and 1 mM sodium orthovanadate, and centrifuged at 100,000g before the supernatant was filtered and loaded onto the indicated affinity resins overnight. After extensive washing, the bound protein was eluted with 3 M NaSCN and salt was removed in Centricon filter units and Excelsior GF-5 detergent removal columns (Pierce) followed by concentration in Microsep 10K filters (Filtron).
 19. M. A. Moses, J. Sudhalter, R. Langer, *Science* **248**, 1408 (1990).
 20. L. Liaw *et al.*, *Circ. Res.* **74**, 214 (1994).
 21. J. Lesley, R. Schulte, R. Hyman, *Exp. Cell Res.* **187**, 224 (1990).
 22. F. P. Reinholt, K. Hultenby, A. Oldberg, D. Heinegard, *Proc. Natl. Acad. Sci. U.S.A.* **87**, 4473 (1990).
 23. T. L. Yue *et al.*, *Exp. Cell Res.* **214**, 459 (1994).
 24. G. F. Weber, S. Abromson-Leeman, H. Cantor, *Immunology* **2**, 363 (1995).
 25. Cells (0.2 × 10⁶) were incubated with biotinylated ligand in 150 μl of calcium- and magnesium-free phosphate-buffered saline (PBS) for 30 min at 37°C followed by fixation in 1% paraformaldehyde for 10 min on ice. After resuspension in calcium- and magnesium-free PBS, phycoerythrin-streptavidin was added at 1:100 dilution for 20 min on ice, and cells were washed and analyzed with a Coulter Profile flow cytometer.
 26. Plates (96 well) were coated with either 10 μg/ml of Opn, 10 μg/ml of fibronectin, or 100 μg/ml of HA for 18 hours at 4°C followed by blocking with 1 mg/ml of BSA (bovine serum albumin) for 2 hours at room temperature. One thousand cells per well were incubated at 37°C in calcium-free and magnesium-free PBS containing 100 μg/ml of BSA. After 30 min the cells were fixed in 4% paraformaldehyde in PBS and stained with toluidine blue. Attachment was assessed by counting the total number of cells per well. Soluble inhibitors were added at the following concentrations: GRGDS peptide, 1 mM; Opn, 500 μg/ml; hyaluronic acid (HA), 1 mg/ml.
 27. A31.MLV or A31.C1 cells (1 × 10⁴ cells/well) in calcium- and magnesium-free PBS were incubated with either 100 μg of HA or 50 μg of Opn for 15 min at 4°C. In experiments with blocking antibody, cells were incubated with CD44 antibody KM 81 (TIB 241 supernatant; 1:20 dilution) for 15 min before addition of ligand. Cells were scored positive when more than 50% of the cells were in aggregates of four or more cells.
 28. J. A. Wass *et al.*, *J. Natl. Cancer Inst.* **66**, 927 (1981).
 29. Surfaces of polycarbonate filters (pore size, 8 μm) were coated with 5 μg of fibronectin before 1 × 10⁵ cells were added in 500 μl to the upper chamber and incubated at 37°C in the presence or absence of chemotactic agents in the lower chamber. After 4 hours, the membranes were fixed in methanol and stained with hematoxylin + toluidine blue. Responding cells on the lower surface of the filter were counted microscopically and evaluated in triplicates.
 30. S. Ashkar *et al.*, *Ann. N.Y. Acad. Sci.* **760**, 296 (1995).
 31. This study was supported in part by NIH research grants AI12184 and AI13600 to H.C.; NIH grant PO1 AR34078 and a grant from the Peabody Foundation to M.J.G.; and a Barr Program Small Grant to G.F.W. J. Schmidt and L. Gerstenfeld provided the K8 osteosarcoma cell line. The authors are grateful to L. Glimcher, C. Rudd, and G. Dranoff for critical reading of the manuscript, to W. Fu for expert technical assistance, and to A. Angel for assistance in the preparation of the manuscript.

8 September 1995; accepted 4 December 1995

Activation by Attention of the Human Reticular Formation and Thalamic Intralaminar Nuclei

Shigeo Kinomura, Jonas Larsson, Balázs Gulyás, Per E. Roland*

It has been known for over 45 years that electrical stimulation of the midbrain reticular formation and of the thalamic intralaminar nuclei of the brain alerts animals. However, lesions of these sectors fail to impair arousal and vigilance in some cases, making the role of the ascending activating reticular system controversial. Here, a positron emission tomographic study showed activation of the midbrain reticular formation and of thalamic intralaminar nuclei when human participants went from a relaxed awake state to an attention-demanding reaction-time task. These results confirm the role of these areas of the brain and brainstem in arousal and vigilance.

Electrical stimulation of the midbrain reticular formation (MRF), an evolutionarily ancient part of the mammalian brainstem (Fig. 1), produces desynchronization in electroencephalograms (EEGs) and awakens and arouses animals (1). Electrocoagulation of this area induces a comatose state and the absence of EEG desynchronization and behavioral arousal to sensory stimuli (2). These observations led to the concept of an ascending reticular activating system and were corroborated by anatomical and electrophysiological studies showing that the MRF sends efferents to the intralaminar

thalamic nuclei. These studies also showed that the MRF and intralaminar nuclei, when stimulated artificially or by sensory stimuli, in concert evoked EEG desynchronization and behavioral arousal and woke up the experimental animals (3, 4).

However, it has been difficult to reproduce the electrocoagulation findings by more refined methods that destroy only the neuronal perikarya of the MRF and not the traversing axons (5). Whereas recordings from MRF neurons have documented the involvement of this part of the brainstem in the transition between sleep and the awake state (6, 7), direct evidence that the MRF and intralaminar nuclei are tonically engaged in maintaining a state of high vigilance and attention has been lacking. We therefore measured the regional cerebral

Division of Human Brain Research, Department of Neuroscience, Karolinska Institute, S-171 77 Stockholm, Sweden.

*To whom correspondence should be addressed.